

Efficient and accurate three-dimensional Poisson solver for surface problems

Luigi Genovese, Thierry Deutsch, and Stefan Goedecker

Citation: *The Journal of Chemical Physics* **127**, 054704 (2007); doi: 10.1063/1.2754685

View online: <http://dx.doi.org/10.1063/1.2754685>

View Table of Contents: <http://scitation.aip.org/content/aip/journal/jcp/127/5?ver=pdfcov>

Published by the [AIP Publishing](#)

Articles you may be interested in

[Efficient and accurate simulation of dynamic dielectric objects](#)

J. Chem. Phys. **140**, 064903 (2014); 10.1063/1.4863451

[Efficient and accurate solver of the three-dimensional screened and unscreened Poisson's equation with generic boundary conditions](#)

J. Chem. Phys. **137**, 134108 (2012); 10.1063/1.4755349

[AQUASOL: An efficient solver for the dipolar Poisson–Boltzmann–Langevin equation](#)

J. Chem. Phys. **132**, 064101 (2010); 10.1063/1.3298862

[Three-dimensional simulation of top down scanning electron microscopy images](#)

J. Vac. Sci. Technol. B **22**, 3399 (2004); 10.1116/1.1825019

[New solutions of the Jacobi equations for three-dimensional Poisson structures](#)

J. Math. Phys. **42**, 4984 (2001); 10.1063/1.1402174



Efficient and accurate three-dimensional Poisson solver for surface problems

Luigi Genovese^{a)} and Thierry Deutsch

Département de Recherche Fondamentale sur La Matière Condensée, SP2M/L_Sim, CEA-Grenoble, 38054 Grenoble Cedex 9, France

Stefan Goedecker

Institute of Physics, University of Basel, Klingelbergstrasse 82, CH-4056 Basel, Switzerland

(Received 26 March 2007; accepted 11 June 2007; published online 6 August 2007)

We present a method that gives highly accurate electrostatic potentials for systems where we have periodic boundary conditions in two spatial directions but free boundary conditions in the third direction. These boundary conditions are needed for all kinds of surface problems. Our method has an $\mathcal{O}(N \log N)$ computational cost, where N is the number of grid points, with a very small prefactor. This Poisson solver is primarily intended for real space methods where the charge density and the potential are given on a uniform grid. © 2007 American Institute of Physics.

[DOI: 10.1063/1.2754685]

I. INTRODUCTION

Electrostatic potentials play a fundamental role in nearly any field of physics and chemistry. Having efficient algorithms to find the electrostatic potential V arising from a charge distribution ρ or, in other words, to solve the Poisson's equation,

$$\nabla^2 V = -4\pi\rho, \quad (1)$$

is therefore essential. The large variety of situations in which this equation can be found lead us to face this problem with different choices of the boundary conditions (BCs). The long-range behavior of the inverse Laplacian operator makes this problem strongly dependent on the BC of the system.

The most immediate approach to the Poisson equation can be achieved for periodic BC, where a traditional reciprocal space treatment is both rapid and simple, since the Laplacian matrix is diagonal in a plane wave representation. If the density ρ is originally given in real space, a first fast Fourier transformation (FFT) is used to transform the real space data in reciprocal space. The Poisson equation is then solved in reciprocal space, and finally the result is transformed back into real space by a second FFT. Because of the FFT's, the overall computational scaling is $\mathcal{O}(N \log N)$ with respect to the number of grid points N .

The situation is different if one considers the same problem for free BC. In this case the solution of Poisson's equation can formally be obtained from a three-dimensional integral,

$$V(\mathbf{r}) = \int d\mathbf{r}' G(|\mathbf{r} - \mathbf{r}'|) \rho(\mathbf{r}'), \quad (2)$$

where $G(r) = 1/r$ is the Green's function of the Laplacian operator in the unconstrained \mathbb{R}^3 space. The long-range nature of the kernel operator G does not allow us to mimic free

BC with a very large periodic volume. Consequently, the description of nonperiodic systems with a periodic formalism always introduces long-range interactions between supercells that falsify the results. Due to the simplicity of the plane wave methods, various attempts have been made to generalize the reciprocal space approach to free BC.¹⁻³ All of them use a FFT at some point and thus have an $\mathcal{O}(N \log N)$ scaling. These methods have some restrictions and cannot be used blindly. For example, the method by Füsti-Molnar and Pulay is efficient only for spherical geometries, and the method by Martyna and Tuckerman requires artificially large simulation boxes that are expensive numerically. Nonetheless, the usefulness of reciprocal space methods has been demonstrated for a variety of applications, and plane wave based codes are widely used in the chemical physics community.

Another choice of the BC that is of great interest is for systems that are periodically replicated in two dimensions but with finite extent in the third, namely, surface systems. The surface-specific experimental techniques developed in recent years produced important results⁴ that can benefit from theoretical prediction and analysis. The development of efficient techniques for systems with such boundary conditions thus became of great importance. Explicit Poisson solvers have been developed in this framework,⁵⁻⁷ with a reciprocal space based treatment. Essentially, these Poisson solvers are built following a suitable generalization for surface BC of the same methods that were developed for isolated systems. As for the free BC case, screening functions are present to subtract the artificial interaction between the supercells in the nonperiodic direction. Therefore, they exhibit the same kind of intrinsic limitations, as, for example, a good accuracy only in the bulk of the computational region, with the consequent need for artificially large simulation boxes which may increase the computational overhead.

Electrostatic potentials can either be calculated by solving the differential Poisson equation or by solving the

^{a)}Electronic mail: luigi.genovese@cea.fr

equivalent integral equation [Eq. (2)]. The methods that solve the differential equation are iterative and they require various tuning. A good representative of these methods is the multigrid approach.⁸ Several different steps such as *smoothing*, *restriction*, and *prolongation* are needed in this approach. Each of these steps has to be tuned to optimize speed and accuracy. Approaches based on the integral equation are in contrast straightforward and do not require such tuning.

In this paper, we will describe a new Poisson solver compatible with the boundary conditions of surfaces. Contrary to Poisson solvers based on reciprocal space treatment, the fundamental operations of this Poisson solver are based on a mixed reciprocal-real space representation of the charge density. This allows us to naturally satisfy the boundary conditions in the different directions. Screening functions or other approximations are thus not needed. For the direction with the free boundary conditions, the guidelines described in Ref. 9 are followed, properly adapted to the surface case.

The charge density in the nonperiodic direction is represented using interpolating scaling functions, thus avoiding from the beginning long-range interactions between supercells. Like the free BC case, this Poisson solver is most efficient when dealing with localized densities (in the nonperiodic direction). Such densities are, for instance, obtained from electronic structure codes using finite differences¹⁰ or finite elements¹¹ or also Gaussians^{12,13} for the representation of the wave functions.

II. INTERPOLATING SCALING FUNCTIONS

Interpolating scaling functions¹⁴ arise in the framework of wavelet theory.^{15,16} They are one-dimensional functions, and their three main properties are as follows:

- The full basis set can be obtained from all the translations by a certain grid spacing h of the mother function ϕ centered at the origin.
- They satisfy the refinement relation

$$\phi(x) = \sum_{j=-m}^m h_j \phi(2x - j), \quad (3)$$

where the h_j 's are the elements of a filter that characterizes the wavelet family, and m is the order of the scaling function. Equation (3) establishes a relation between the scaling functions on a grid with grid spacing h and another one with spacing $h/2$.

- The mother function ϕ is symmetric, with compact support from $-m$ to m . It is equal to 1 at the origin and to 0 at all other integer points (in grid spacing units). The expansion coefficients of any function in this basis are just the values of the function on the grid.

III. POISSON EQUATION FOR SURFACE BC

Consider a three-dimensional domain, periodic (with period L_x and L_y) in x and y directions and nonperiodic in z . Without loss of generality, a function f that lives in such a domain can be expanded as

$$f(x, y, z) = \sum_{p_x, p_y} e^{-2\pi i((p_x/L_x)x + (p_y/L_y)y)} f_{p_x, p_y}(z). \quad (4)$$

We indicate with $f_{p_x, p_y}(z)$ the one-dimensional function associated with the vector $\mathbf{p} = (p_x/L_x, p_y/L_y)$ in the reciprocal space of the two-dimensional surface. Following these conventions, the Poisson equation [Eq. (1)] becomes a relation between the reciprocal space components of V and ρ ,

$$V_{p_x, p_y}(z) = -4\pi \int_{-\infty}^{+\infty} dz' G(2\pi|\mathbf{p}|; z - z') \rho_{p_x, p_y}(z'), \quad (5)$$

where $|\mathbf{p}|^2 = (p_x/L_x)^2 + (p_y/L_y)^2$, and $G(\mu; z)$ is the Green's function of the one-dimensional Helmholtz equation,

$$(\partial_z^2 - \mu^2)G(\mu; z) = \delta(z). \quad (6)$$

The free BC on the z direction fixes the form of the Green's function,

$$G(\mu; z) = \begin{cases} -(1/2\mu)e^{-\mu|z|}, & \mu > 0 \\ (1/2)|z|, & \mu = 0. \end{cases} \quad (7)$$

In numerical calculations continuous charge distributions are typically represented by their values on a grid. The mixed representation of the charge density given above immediately suggests to use a plane wave expansion in the periodic directions, which may be easily treated with conventional FFT techniques. For the nonperiodic direction z , we will use the interpolating scaling function representation. The corresponding continuous charge distribution is thus given by

$$\rho(x, y, z) = \sum_{p_x=-N_x/2}^{N_x/2} \sum_{p_y=-N_y/2}^{N_y/2} \sum_{j_z=0}^{N_z} \rho_{p_x, p_y; j_z} \times \exp\left(-2\pi i\left(\frac{p_x}{L_x}x + \frac{p_y}{L_y}y\right)\right) \phi\left(\frac{z}{h} - j_z\right), \quad (8)$$

where h is the grid spacing in the z direction, and $\phi(j) = \delta_{j,0}$, $j \in \mathbb{Z}$. This mixed representation of the charge density in Eq. (8) has an important property. It is in a certain sense the most faithful continuous charge distribution that can be obtained from values on a grid. The main features of the electrostatic potential are determined by the multipoles and Fourier components of the charge distribution. For surface problems the multipoles are the significant quantity along the nonperiodic direction and the Fourier components are the relevant quantities in the two periodic directions. Using the completeness relation of plane waves (which holds also on a discrete real space grid) and the relation

$$\int dx \phi(x - j) x^\ell = j^\ell, \quad (9)$$

which is demonstrated in Ref. 9, it is easy to show that

$$\begin{aligned}
& \int dx dy dz \cos\left(\frac{2\pi\ell_1 x}{L_x}\right) \cos\left(\frac{2\pi\ell_2 y}{L_y}\right) z^{\ell_3} \rho(x, y, z) \\
&= \frac{L_x L_y h^{\ell_3+1}}{4} \sum_{\epsilon_{1,2}=\pm 1} \sum_{j_3=0}^{N_z} j_3^{\ell_3} \rho_{\epsilon_1 \ell_1, \epsilon_2 \ell_2; j_3} \\
&= L_x L_y h^{\ell_3+1} \sum_{j_1=0}^{N_x} \sum_{j_2=0}^{N_y} \sum_{j_3=0}^{N_z} \\
&\quad \times \cos\left(\frac{2\pi\ell_1 j_1}{N_x}\right) \cos\left(\frac{2\pi\ell_2 j_2}{N_y}\right) j_3^{\ell_3} \rho\left(\frac{L_x}{N_x} j_1, \frac{L_y}{N_y} j_2, h j_3\right),
\end{aligned} \tag{10}$$

with $\ell_1 < N_x$, $\ell_2 < N_y$, and $\ell_3 < m$, where m is the order of the scaling function. This equation shows that the discrete multipoles and Fourier components of a charge density given on a grid are identical to the multipoles and Fourier components of the continuous ρ given by Eq. (8). For this reason it is not necessary that the input charge density for our method is given in the representation of Eq. (8). It can, and it will actually in most cases, be given by numerical values on a grid.

Combining Eq. (5) with Eq. (8), the discretized Poisson problem thus becomes

$$V_{p_x, p_y, j_z} = -4\pi h \sum_{j'_z} K(2\pi|\mathbf{p}|; j_z - j'_z) \rho_{p_x, p_y, j'_z}, \tag{11}$$

where the quantity (kernel)

$$K(\mu; j) = \int_{-\infty}^{+\infty} du G(\mu; h(j-u)) \phi(u) \tag{12}$$

is defined via an integral in the dimensionless variable u . Due to the symmetry of ϕ , the kernel is symmetric in the nonperiodic direction $K(\mu; j_z) = K(\mu; -j_z)$. The integral bounds can be restricted from $-m$ to m , thanks to the compact support of ϕ .

Once we have calculated the kernel, which will be described below, our numerical procedure is the following. We perform a two-dimensional FFT on our real space charge density to obtain the Fourier coefficients ρ_{p_x, p_y, j'_z} for all the periodic planes. Then we have to solve Eq. (11). Since this equation is a convolution, it can be calculated by zero-padded FFT's. Finally, the potential is transformed back from the mixed representation to real space to obtain the potential on the grid by another two-dimensional FFT. Due to the FFT's, the total computational cost is $\mathcal{O}(N \log N)$. Since all quantities are real, the amount of memory and the number of operations for the FFT can be reduced by using real-to-complex FFT's instead of complex-complex FFT's.

All that remains to be done now is to calculate the values of the kernel function $K(\mu; j)$. The core of the calculation is represented by the function

$$\tilde{K}(\lambda; j) = \begin{cases} \int du e^{-\lambda|u-j|} \phi(u), & \lambda > 0 \\ \int du |u-j| \phi(u), & \lambda = 0. \end{cases} \tag{13}$$

The kernel has the properties $K(\mu; j) = -\tilde{K}(\mu h; j)/(2\mu)$ for $\mu > 0$ and $K(0; j) = \tilde{K}(0; j)/2$. A simple numerical integration

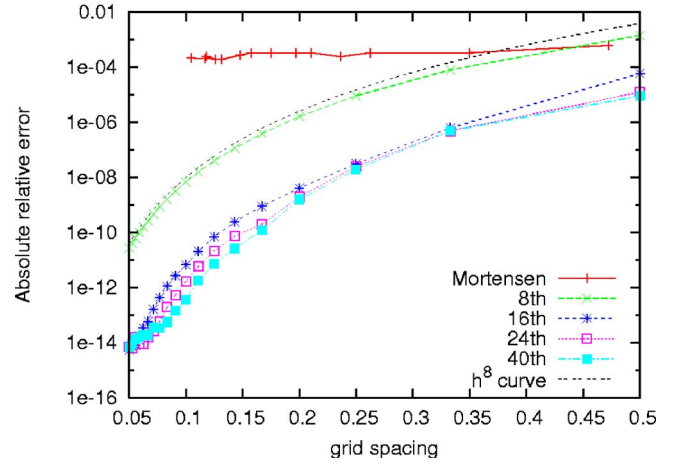


FIG. 1. (Color online) Accuracy comparison between our method with scaling functions of different orders and the Mortensen solver for surface systems as implemented in CPMD. The results of the Hockney method are not shown since they are much less precise. The h^8 curve is plotted to show the algebraic decrease of the precision with respect to the grid space h . The accuracy is finally limited by the evaluation of integral (13), which is computed with nearly machine precision.

with the trapezoidal rule is inefficient since $G(\mu; z)$ is not smooth in $z=0$, while the scaling function varies significantly around the integer points. Thanks to the compact support of the scaling function, this problem can be circumvented with a simple and efficient recursive algorithm. We define two functions $\tilde{K}^{(+)}$ and $\tilde{K}^{(-)}$ such that $\tilde{K}(\lambda; j) = \tilde{K}^{(+)}(\lambda; j) + \tilde{K}^{(-)}(\lambda; j)$, where we have, for $\lambda > 0$,

$$\tilde{K}^{(+)}(\lambda; j) = \int_{-\infty}^j du e^{\lambda(u-j)} \phi(u), \tag{14}$$

$$\tilde{K}^{(-)}(\lambda; j) = \int_j^{+\infty} du e^{-\lambda(u-j)} \phi(u), \tag{15}$$

while with $\lambda=0$,

$$\tilde{K}^{(\pm)}(0; j) = \pm j Z_0^{(\pm)}(j) \mp Z_1^{(\pm)}(j), \tag{16}$$

$$Z_\ell^{(+)}(j) = \int_{-\infty}^j du u^\ell \phi(u), \tag{17}$$

$$Z_\ell^{(-)}(j) = \int_j^{+\infty} dx u^\ell \phi(u), \quad \ell = 0, 1. \tag{18}$$

These objects satisfy recursion relations

$$\tilde{K}^{(\pm)}(\lambda; j+1) = e^{\mp\lambda} [\tilde{K}^{(\pm)}(\lambda; j) \pm e^{\mp\lambda j} D_\lambda^{(\pm)}(j)], \tag{19}$$

$$Z_\ell^{(\pm)}(j+1) = Z_\ell^{(\pm)}(j) \pm C_\ell(j), \quad \ell = 0, 1,$$

where

$$D_\lambda^{(\pm)}(j) = \int_j^{j+1} du e^{\pm\lambda u} \phi(u), \tag{20}$$

TABLE I. Evaluation error of the Hartree energy (hartree) for different values of the size L of the nonperiodic direction, for a system with an electrostatic density which is localized in the nonperiodic direction with characteristic length L_0 . The density of this system is identical to the one used for the accuracy tests of Fig. 1, with $2L_0=L_z$ (see text). The accuracy of the Mortensen approach with $L=2L_0$ is of the same order of the accuracy obtained by our approach with $L=L_0$, which means that to obtain the same precision with Mortensen method the size of the system must be roughly doubled.

L_0/L	0.5	0.6	0.7	0.8	0.9	1
$m=14$	1×10^{-12}	7×10^{-12}	4×10^{-6}	2×10^{-3}	3×10^{-2}	2×10^{-1}
Mortensen	0.2	1.3	3.7	6.0	6.8	6.2

$$C_\ell(j) = \int_j^{j+1} du u^\ell \phi(u), \quad \ell = 0, 1. \quad (21)$$

From Eqs. (14)–(21) and the properties

$$\begin{aligned} \tilde{K}(\lambda; j) &= \tilde{K}(\lambda; -j), \quad \tilde{K}^{(+)}(\lambda; 0) = \tilde{K}^{(-)}(\lambda; 0), \\ Z_1^{(+)}(0) &= Z_1^{(-)}(0), \quad Z_0^{(+)}(0) = Z_0^{(-)}(0) = \frac{1}{2}, \end{aligned} \quad (22)$$

the function $\tilde{K}(\lambda; j)$ can be calculated recursively for each $j \in \mathbb{N}$, by knowing $\tilde{K}^{(+)}(\lambda; 0)$ and $Z_1^{(+)}(0)$, then evaluating $D_\lambda^{(\pm)}(j)$ and $C_\ell(j)$ for each value of j . The integrals involved can be calculated with high accuracy with a simple higher order polynomial quadrature. They are integral of smooth, well-defined quantities, since the interpolating scaling function goes to zero at their bounds. Moreover, for values of j lying outside the support of ϕ , we can benefit of a functional relation for calculating the values of the kernel. The support of an m th order scaling function goes from $-m$ to m , then we have $\forall p > 0$,

$$\begin{aligned} K(\mu; m+p) &= e^{-\mu hp} K(\mu; m), \quad \mu > 0, \\ K(0; m+p) &= K(0; m) + p Z_0^{(+)}(m). \end{aligned} \quad (23)$$

To summarize, we have found an efficient method for evaluating Eq. (12) for $j=0, \dots, N_z$ and a fixed μ . Instead of calculating N_z+1 integrals of range $2m$, we can obtain the same result by calculating two integrals of range m and $4m$ integrals of range 1, with the help of relation (23). This will also increase accuracy, since the integrands are always smooth functions, which would not be the case with a naive approach.

The accuracy in calculating the integrals can be further improved by using refinement relation (3) for interpolating scaling functions. For positive λ we have

$$\begin{aligned} \tilde{K}(2\lambda; i) &= \int du e^{-2\lambda|u-i|} \phi(u) \\ &= \frac{1}{2} \int du e^{-\lambda|u-2i|} \phi(u/2) \\ &= \frac{1}{2} \sum_j h_j \int du e^{-\lambda|u-2i|} \phi(u-j) \\ &= \frac{1}{2} \sum_j h_j \tilde{K}(\lambda; 2i-j). \end{aligned} \quad (24)$$

This relation is useful to improve the accuracy in evaluating

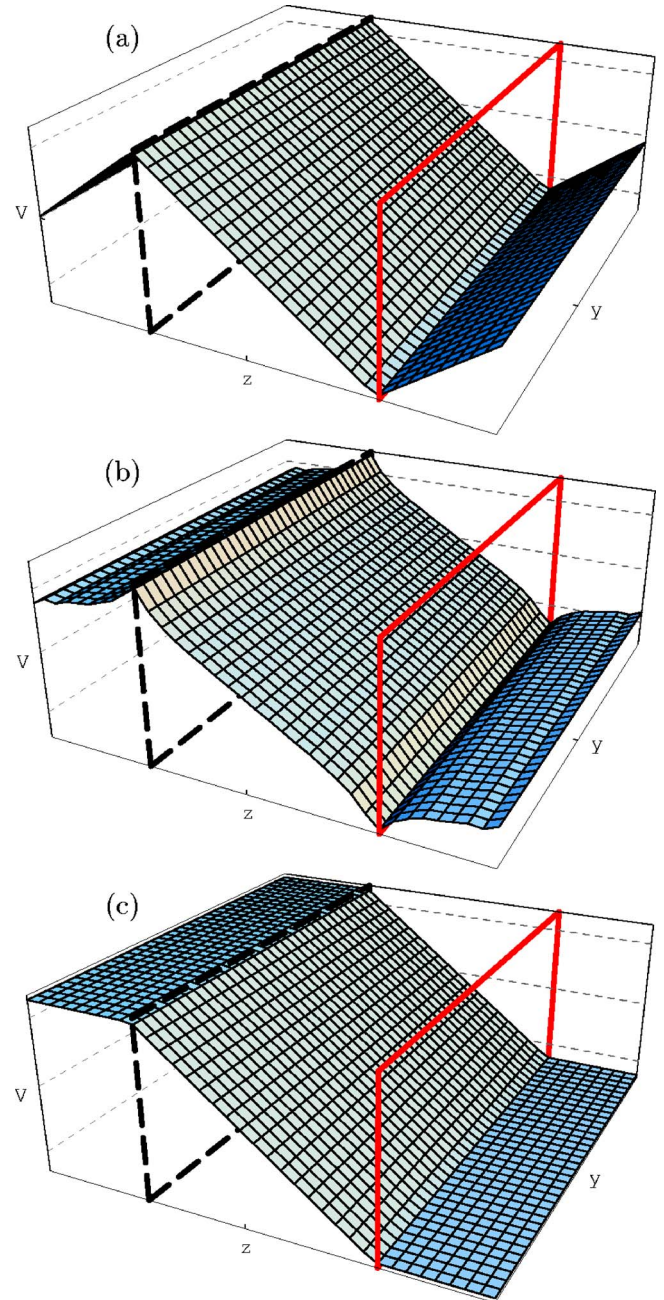


FIG. 2. (Color online) Electrostatic potential V for a system with two periodic planes charged with opposite sign (plane capacitor), oriented along the z direction, calculated by different Poisson solvers. The values of V are taken in the middle of the x (periodic) direction. The position of the positive (black, dashed line) and the negative (red, solid) charged plane is schematically shown in the figure. The represented solutions are, from top to bottom, the results from the Mortensen, the Hockney, and our Poisson solver.

TABLE II. The elapsed time in seconds required on a Cray XT3 (based on AMD Opteron processors) to solve Poisson's equation with surface BC on a 128^3 grid as a function of the number of processors. The time for setting up the Kernel (around 50% of the total time) is not included. For a large number of processors, the communication time needed to gather the complete potential to all the processors becomes dominant.

1	2	4	8	16	32	64	128
0.43	0.26	0.16	0.10	0.07	0.05	0.04	0.03

the kernel for high λ . Since in this case the exponential function is very sharp, it is better to calculate the kernel for lower λ and an enlarged domain and then apply relation (24) as many times as needed. Relation (23) allows us to enlarge the domain with no additional computational cost. With the help of the above described properties, the computational time for evaluating the kernel in Fourier space can be considerably optimized, becoming roughly half of the time needed for its application on a real space density.

IV. NUMERICAL RESULTS AND COMPARISON WITH OTHER METHODS

Our new method has an algebraic convergence rate of h^m , where h is the grid spacing and m is the order of the interpolating scaling function used. This is due to the fact that the charge density along the nonperiodic direction can be represented with an approximation error of the order of h^m using interpolating scaling functions of order m .¹⁶ The error of the plane wave representation of the charge density in the periodic plane has a faster exponential convergence rate and is thus not visible in the overall convergence rate. By choosing higher order interpolating scaling function, we can get arbitrarily high algebraic convergence rates. From a computational point of view, this will result in increasing the number of operations to perform for calculating the kernel function. In the previous section we saw that both the calculation of the integral of Eq. (13) and the evaluation of recursion relation (24) require a number of operations which is linear in m . Consequently, the overall scaling of the number of operations is of order m^{r+1} , where r is the maximum number of nested applications of Eq. (24) in the calculation. Such scaling is, however, purely theoretical, since the prefactor is so little that other parts of the calculations (e.g., the kernel FFT) will result to be dominant. Moreover, with values of m reasonably little we can easily attain machine precision. Our method was compared with the reciprocal space methods by Hockney and Eastwood⁷ and Mortensen and Parrinello⁶ (which is a suitable generalization for two-dimensional slab geometries of the method described in Ref. 2) as implemented in the CPMD electronic structure program.¹⁷ The accuracy tests shown in Fig. 1 are performed with an analytical charge distribution that is the Laplacian of $V(x,y,z) = \exp(\cos((2\pi/L_x)x) + \cos((2\pi/L_y)y))\exp(-(z^2/50L_z^2) - \tan((\pi/L_z)z)^2)$. Its behavior along the xy surface is fully periodic, with all the reciprocal space components taken into account. The $\exp(-\tan((\pi/L_z)z)^2)$ guarantees a localized behavior in the nonperiodic direction with the potential going explicitly to zero at the borders. This makes also this function suitable for comparison with the reciprocal space based approach. The Gaussian factor is added to suppress high fre-

quency components. Tests with other analytical functions gave comparable accuracies. The reciprocal space Poisson solvers turn out to be much less precise than our approach, which explicitly preserves the BC along each direction. Moreover, the accuracy shown for the Mortensen approach is calculated only for planes that lie in the bulk of the nonperiodic direction (30% of the total volume). Outside of this region, errors in the potential blow up. Table I shows the behavior of the errors in computing the Hartree energy following the size of the system in the nonperiodic direction. To obtain the same accuracy of our approach with the Mortensen method, we need a system which is roughly twice larger, which will imply that a very large computational volume is needed to obtain accurate results in a sufficiently large domain of the nonperiodic direction.

To show that our method genuinely preserves the boundary conditions appropriate for surfaces, we calculated the electrostatic potential for a plane capacitor. For this system only the zeroth Fourier components in the plane are nonvanishing. Figure 2 shows the results either in the Mortensen/Hockney reciprocal space methods or with our approach. For the plane capacitor, the screening function used in the Mortensen approach vanishes, and the solution is equal to what we would have obtained with fully periodic boundary conditions. To obtain the good "zero electric field" behavior in the borders that we obtain directly with our method, one would have to postprocess the solution obtained from the Mortensen method, by adding to the potential a suitable linear function along the nonperiodic direction. This is legitimate since a linear function is annihilated by the Laplace operator and the modified potential is thus also a valid solution of the Poisson equation just with different boundary conditions. The Hockney method presents a better qualitative behavior, though the results are not accurate. Only with our approach we get both accurate and physically sound results.

Table II shows the required CPU time for solving the Poisson equation on a grid of 128^3 grid points as a function of the number of processors on a Cray XT3 parallel computer. The parallel version is based on a parallel three-dimensional FFT, where the input/output is properly distributed/gathered to all the processors. The FFT's are performed using a modified version of the algorithm described in Ref. 18 that gives high performances on a wide range of computers.

A package for solving Poisson's equation in real space according to the method described here can be downloaded.¹⁹

In conclusion, we have presented a method that allows us to obtain accurate potentials arising from charge distributions on surfaces with an $\mathcal{O}(N \log N)$ scaling in a mathemati-

cally clean way. This method preserves explicitly the required boundary conditions and can easily be used for applications inside electronic structure codes where the charge density is either given in reciprocal or in real space.

ACKNOWLEDGMENTS

The authors acknowledge interesting discussions with François Bottin and Jaroslaw Piwonski. This work was supported by the European Commission within the Sixth Framework Program through NEST-BigDFT (Contract No. BigDFT-511815) and by the Swiss National Science Foundation. The timings were performed at the CSCS (Swiss Supercomputing Center) in Manno.

¹R. W. Hockney, *Methods Comput. Phys.* **9**, 135 (1970).

²G. J. Martyna and M. E. Tuckerman, *J. Chem. Phys.* **110**, 2810 (1999).

³L. Füsti-Molnar and P. Pulay, *J. Chem. Phys.* **116**, 7795 (2002).

⁴M.-C. Desjonquères and D. Spanjaard, *Concepts in Surface Physics*, Springer Series in Surface Sciences (Springer-Verlag, Berlin, 1998).

⁵P. Minary, M. E. Tuckerman, K. A. Pihakari, and G. J. Martyna, *J. Chem. Phys.* **116**, 5351 (2002).

⁶J. J. Mortensen and M. Parrinello, *J. Phys. Chem. B* **104**, 2901 (2000).

⁷R. W. Hockney and J. W. Eastwood, *Computer Simulation Using Particles* (McGraw-Hill, New York, 1981).

⁸W. Hackbusch and U. Trottenberg, *A Multigrid Method* (Springer, Berlin, 1982).

⁹L. Genovese, T. Deutsch, A. Neelov, S. Goedecker, and G. Beylkin, *J. Chem. Phys.* **125**, 074105 (2006).

¹⁰J. R. Chelikowsky, N. Troullier, and Y. Saad, *Phys. Rev. Lett.* **72**, 1240 (1994).

¹¹J. E. Pask, B. M. Klein, C. Y. Fong, and P. A. Sterne, *Phys. Rev. B* **59**, 12352 (1999).

¹²J. VandeVondele, M. Krack, M. Fawzi, M. Parrinello, T. Chassaing, and J. Hutter, *Comput. Phys. Commun.* **167**, 103 (2005).

¹³G. Lippert, J. Hutter, and M. Parrinello, *Mol. Phys.* **92**, 477 (1997).

¹⁴G. Deslauriers and S. Dubuc, *Constructive Approx.* **5**, 49 (1989).

¹⁵I. Daubechies, *Ten Lectures on Wavelets* (SIAM, Philadelphia, 1992).

¹⁶S. Goedecker, *Wavelets and Their Application For The Solution of Partial Differential Equations* (Presses Polytechniques Universitaires et Romandes, Lausanne, 1998).

¹⁷J. Hutter, A. Alavi, T. Deutsch, M. Bernasconi, S. Goedecker, D. Marx, M. Tuckerman, and M. Parrinello, CPMD, Version 3.8, Max-Planck-Institut für Festkörperforschung and IBM Zürich Research Laboratory, 1995–1999.

¹⁸S. Goedecker, *Comput. Phys. Commun.* **76**, 294 (1993).

¹⁹<http://www.unibas.ch/comphys/comphys/SOFTWARE>